

Orchestrated increase of dopamine and PARK mRNAs but not miR-133b in dopamine neurons in Parkinson's disease[☆]



Falk Schaudraff^a, Jan Gründemann^{b,1}, Michael Fauler^{a,1}, Elena Dragicevic^a, John Hardy^c, Birgit Liss^{a,*}

^a Department of Applied Physiology, Institute of Applied Physiology, University of Ulm, Ulm, Germany

^b Friedrich Miescher Institute for Biomedical Research, Basel, Switzerland

^c Department of Molecular Neuroscience and Reta Lila Weston Laboratories, Institute of Neurology, London, UK

ARTICLE INFO

Article history:

Received 6 August 2013

Received in revised form 27 February 2014

Accepted 14 March 2014

Available online 22 March 2014

Keywords:

SNCA140
PARK
RIN
Mixed-effects-model
miR-133b
NURR1
PITX3
UV-LMD
UCHL-1
ATPase13A2
Parkin
LRRK2

ABSTRACT

Progressive loss of substantia nigra dopamine neurons (SN DA) is a hallmark of aging and of Parkinson's disease (PD). Mutations in PARK genes cause familial PD forms. Increased expression of alpha-synuclein (PARK4) is a disease-triggering event in familial PD and also observed in SN DA neurons in sporadic PD but related transcriptional changes are unknown. With optimized single-cell quantitative real-time polymerase chain reaction analysis, we compared messenger RNA and microRNA levels in SN DA neurons from sporadic PD patients and controls. Non-optimally matched donor ages and RNA integrities are common problems when analyzing human samples. We dissected the influence of distinct ages and RNA integrities of our samples by applying a specifically-optimized, linear-mixed-effects model to quantitative real-time polymerase chain reaction-data. We identified that elevated alpha-synuclein messenger RNA levels in SN DA neurons of human PD brains were positively correlated with corresponding elevated levels of mRNAs for functional compensation of progressive SN DA loss and for enhanced proteasomal (PARK5/UCHL1) and lysosomal (PARK9/ATPase13A2) function, possibly counteracting alpha-synuclein toxicity. In contrast, microRNA miR-133b levels, previously implicated in transcriptional dysregulation in PD, were not altered in SN DA neurons in PD.

© 2014 The Authors. Published by Elsevier Inc. All rights reserved.

1. Introduction

Parkinson's disease (PD) is the second most common neurodegenerative disorder. Since the main risk factor for the disease is age, the number of PD patients is projected to further increase worldwide (Hindle, 2010). Current pharmaceutical and neurosurgical therapies provide only symptomatic treatment with no cure available (Meissner et al., 2011). Clinical core symptoms of PD are caused by a selective degeneration of dopamine (DA) midbrain neurons, particularly within the substantia nigra (SN), resulting in a dopamine deficit in striatal target regions (Shulman et al., 2011). Loss of DA neurons is usually preceded by a cellular accumulation of alpha-

synuclein-positive protein conglomerates, so-called Lewy bodies (Spillantini et al., 1997). The cause for PD is still unclear, however mitochondrial, proteasomal as well as lysosomal dysfunctions are relevant triggers (Gasser et al., 2011). Depending on the ethnic population, approximately 10%–30% of familial forms of PD are caused by mutations in one of the several PARK gene loci (PARK1–15) (Shulman et al., 2011).

In sporadic PD cases, simple Mendelian inheritance patterns are not observed. Genome-wide analysis of single-nucleotide polymorphisms or copy number variations identified an increasing number of disease-associated genes (Gasser et al., 2011; Hardy, 2010; Nalls et al., 2011). However, a PD risk prediction based on validated single-nucleotide polymorphisms is not yet possible (Mittag et al., 2012). The major validated genetic factor for sporadic PD is the SNCA gene (Pihlstrom and Toft, 2011). SNCA codes for the protein alpha-synuclein and was the first gene (PARK1) identified to be mutated in familial forms of PD (Polymeropoulos et al., 1997). Full functions of the alpha-synuclein tetramer are still not clear, however, it is involved in vesicular trafficking and dopamine release

[☆] This is an open access article under the CC BY-NC-ND license (<http://creativecommons.org/licenses/by-nc-nd/3.0/>).

* Corresponding author at: Institute of Applied Physiology, University of Ulm, Albert Einstein Allee 11, 89081 Ulm, Germany. Tel.: +49 (0)731 500 36200; fax: +49 (0)731 500 36202.

E-mail address: birgit.liss@uni-ulm.de (B. Liss).

¹ These authors contributed equally to distinct aspects of the article.

(George et al., 2013; Kalia et al., 2013). Transcriptional upregulation of nonmutated wild-type alpha-synuclein because of SNCA gene duplications or triplications (PARK4) is sufficient to cause familial forms of PD (Fuchs et al., 2007). Furthermore, elevated levels of alpha-synuclein messenger RNA (mRNA) in substantia nigra dopamine neurons (SN DA) neurons have been observed in sporadic PD (Grundemann et al., 2008; Shulman et al., 2011; Venda et al., 2010). These findings point to a key role of wild-type SNCA gene-dosage for death of DA neurons in sporadic PD (Devine et al., 2011b; Eriksen et al., 2005). Thus, identifying transcripts that co-vary in their expression levels with that of SNCA provide strong evidence for alpha-synuclein-linked pathways that are operative in SN DA neurons of sporadic PD patients and contribute to PD pathology. However, cell-specific alpha-synuclein associated changes in gene expression that occur specifically in human SN DA neurons, the most vulnerable neuronal population in PD, are still unknown.

We performed cell-specific gene expression analysis of selected genes for individual human SN DA neurons from sporadic PD brains and controls. Given the emerging role of microRNAs for orchestrating correlated transcriptional programs, and the suggestion that miR-133b has a prominent role for those programs and in PD (Harratz et al., 2011; Kim et al., 2007), we developed a RT-qPCR protocol for parallel quantification of both mRNA and microRNA at the level of individual, ultra violet-laser-microdissected (UV-LMD) neurons from human postmortem brains. For human samples, optimal matching is commonly not possible, causing a general problem for gene expression comparison at the RNA level: differences in co-factors that have a biological (e.g. different ages) or methodological (e.g. different RNA integrities) impact on results, and thus confound comparative gene expression analysis (e.g. comparison disease vs. controls). To adjust gene expression data for possible influences of distinct ages and RNA integrity numbers (RIN) of human control and PD brain samples (present in our cohort), we developed a suited linear mixed 3-effects algorithm (Greenland and Morgenstern, 2001), that has not been applied to gene expression data before (Ho-Pun-Cheung, 2009; Popova et al., 2008), to dissect the influence of distinct ages and RNA integrities of our samples to the RT-qPCR results in addition to disease state (PD vs. control).

We show that neuromelanine-positive SN DA neurons from sporadic PD brains with significantly elevated SNCA mRNA levels exhibit a concerted upregulation of distinct dopamine homeostasis and PARK genes. The positive correlation of mRNA levels with that of SNCA in SN DA neurons points to an orchestrated allostatic dysregulation at the mRNA level in PD. In contrast, we detected no associated change of miR-133b levels in individual SN DA neurons in PD.

2. Methods

2.1. Tissue storage and preparation of midbrain sections for UV-laser microdissection

Details for all 13 human postmortem horizontal midbrain tissue blocks (provided by the German BrainNet, Grant-No. GA 28, and Dietmar R. Thal, University of Ulm, Germany) are given in Table 1. Murine tissue samples for control experiments derived from male C57BL/6 J WT mice (PN 19). Murine and human midbrain tissue cryoconservation, handling, sectioning, fixation, and staining were performed as previously described (Grundemann et al., 2008, 2011).

2.2. Tissue pH measurements, tissue RNA extraction, and RIN analysis

pH measurements of human postmortem midbrain tissue samples were performed with a pH Optica micro system and a MicroTip fiber optic pH sensor (World Precision Instruments, Sarasota, FL,

USA) calibrated at 4 °C (Harrison et al., 1995; Mexal et al., 2006). Frozen cryosections (12 µm) of each midbrain were harvested, 10 µL of 4 °C cold molecular biology grade water (Eppendorf) were added per mg tissue and samples were homogenized using a sterile 1 mL syringe and a 21-gauge needle. pH was measured at 4 °C. Total RNA of human postmortem horizontal midbrain tissue cryosections was extracted using the RNeasy Mini Kit (Qiagen). For RNA quality control, RNA integrity numbers (RINs) were determined using the Agilent 2100 Bioanalyzer system with the Agilent RNA 6000 Nano Chip Kit. Small RNA fractions and microRNA percentage were determined using the Agilent Small RNA Kit.

2.3. UV-LMD, reverse transcription, and RT-qPCR

UV-LMD and quantitative real-time PCR were performed essentially as described (Grundemann et al., 2008, 2011). qPCR methods and data are provided according to the “Minimal Information for Publication of Quantitative Real-Time PCR Experiments (MIQE) guidelines” (Pihlstrom and Toft, 2011). For all details, see [Supplementary methods](#). Briefly, 10 pools of 15 neuromelanine-positive (NM⁺) SN neurons each were harvested from each individual midbrain via UV-LMD (Leica LMD6000) for each gene expression profiling experiment. For parallel qPCR quantification of miR-133b and mRNA, the miScript Reverse Transcription Kit (Qiagen) was used. A 1/11 volume of the non-purified complementary DNA (cDNA) was used as a template for each real-time qPCR in a final volume of 20 µL (TaqMan), using 1 × QuantiTect Probe PCR Master Mix (Qiagen). All real-time qPCR assays were labeled with 6-carboxyfluorescein (FAM) as reporter and a nonfluorescent quencher (BHQ). Real-time qPCR assay details, amplicons and assay-specific standard curve parameters, threshold for cycle analysis, and slopes and Y-intercept of respective standard curves: see [Supplementary Table S1](#).

For thermal degradation assay, distinct RINs of the same RNA sample (mouse midbrain) were generated by incubation of RNA sample at 70 °C for 30 minutes (RIN 7.2), 45 minutes (RIN 6.8), and 72 minutes (RIN 5.9).

Relative expression data of midbrain tissue RT-qPCR data ([Supplementary Table S3](#)) were normalized by the geometric mean from β-actin, TIF-1A, and ENO2 expression:

Normalized cDNA amount in SN tissue

$$= \frac{S^{(Ct - Y)/s}}{\sqrt[3]{S \sum \frac{Ct_i - Y_i}{s_i}}} \text{ with } i \in \{\beta\text{-actin, TIF-1A, ENO2}\}$$

2.4. Linear mixed effects modeling and adjustment of expression data to covariates

To adjust for possible confounding influence of other variables (in particular age and RIN) on gene expression differences between control and PD samples, a hierarchical, multivariate linear mixed effects model with a multi-trait design was fitted to each of the 5 independent RT-qPCR data sets by applying Asreml-R (version 3.0, VSN International) in the R environment (version 2.15, The R-Project for statistical computing). Details of the model, its evaluation, and the full algorithm are given in the [Supplementary methods, Figures, and Tables](#).

Briefly, expression values of distinct analyzed genes, determined via RT-qPCR assays, were defined as different traits, coupled by an unstructured covariance matrix and similar influence of RNA integrity as measured by RIN values. Random effects for gene dependent Y-intercepts, incorporated at the brain level, accounted for the hierarchical design of the study (cell samples, brains, and control or disease group), and for inter-individual differences in gene

Table 1
Details of human control and PD brain tissue

Code-number	Disease state	CERAD	Braak (AD)	Age (years), sex	PMI (h)	pH	RIN	Small RNA (ng/ μ L)	Amount miRNA (%)
Controls									
CTR-SN 1	Hypertonia, coronary infarction	0	I	62, M	31	5.9	6.2	5.08	28
CTR-SN 2	CMV, diabetes, nephritis kidney transplant	0	II	72, M	6	6.4	6.6	5.91	26.3
CTR-SN 3	Diabetes, hypertonia, pneumonia, ARDS	A	I	69, F	14	6.6	6.5	11.02	17
CTR-SN 4	Arteriosclerosis	0	I	75, F	24	5.5	6	13.07	19.7
CTR-SN 5	Liver cancer, hepatorenal syndrome	0	0	63, M	24	6	6.3	8.01	26.5
Mean (\pm SEM) controls (1–5)				68.2 \pm 2.52	19.8 \pm 4.39	6.08 \pm 0.19	6.32 \pm 0.12	8.62 \pm 1.51	23.5 \pm 2.16
CTR-SN 6 ^a	Sepsis, mamma carcinoma, CNS micro abscesses	0	II	68, F	120	5.7	5.9	7.1	28.6
CTR-SN 7 ^a	Cervix carcinoma, arterial hypertonia, COPD, pulmonary embolism, old frontal micro infarct	0	I	71, F	72	5.67	6.5	5.62	21.3
CTR-SN 8 ^a	Lymphoma-NHL-high malignancy, Bergmann cell gliosis	0	I	72, M	24	5.65	6.6	8.26	31.6
Mean controls (1–8)				69 \pm 1.6	39.38 \pm 13.43	5.93 \pm 0.14	6.3 \pm 0.1	8 \pm 0.98	24.88 \pm 1.77
PDs									
PD-SN 1	PD, multi system atrophy	0	II	80, M	7	6.4	7.1	3.66	11.3
PD-SN 2	PD, AD1, hypertonia pneumonia	B	III–IV	80, M	23	5.4	6.8	9.24	15.2
PD-SN 3	PD	0	II	79, F	17	5.8	7.3	3.08	12.1
PD-SN 4	PD, AD, heart attack, lung carcinoma	0	0	79, M	23	6.2	7.5	3.06	12.5
PD-SN 5	PD, ovarian cancer, Morbus Sudeck	0	V	73, F	11	5.5	7.7	5.62	19.8
Mean PDs				78.2 \pm 1.3	16.2 \pm 3.2	5.86 \pm 0.19	7.28 \pm 0.16	4.93 \pm 1.17	14.18 \pm 1.55

Details of all 13 human midbrain samples are used in this study. Listed for each brain are: additional known diseases, CERAD (Consortium to Establish a Registry for Alzheimer's Disease) stage, Braak stage (concerning AD—Alzheimer's disease), age of donor in years (a), sex (M: male, F: female), postmortem interval (PMI), pH of brain tissue, RNA integrity number (RIN), and amount of small RNAs with fraction of miRNA (%).

Mean \pm SEM values and significant differences ($p < 0.05$, marked in bold) are given for the cohort of control and PD brains.

Key: AD, Alzheimer's disease; ARDS, acute respiratory distress syndrome; CMV, cytomegalie-virus; CNS, central nervous system; COPD, chronic obstructive lung disease; F, female; M, male; miRNA, microRNA; NHL, non-Hodgkin-lymphoma; PD, Parkinson's disease.

^a CTR-SN controls are not included in experimental series random 1, 2 and miScript 5; PD-SN sporadic Parkinson's disease cases.

expression. The chosen model structure, with regard to incorporated covariates, was selected on the basis of model performances, quantified by the Bayesian Information Criterion (BIC, [Supplementary Fig. 1A](#)) and the biological or experimental relevance of possible confounds ([Fig. 1A](#)). BIC values were computed for single-trait models (TH gene only) of different complexity with the lme function of the nlme R-package by maximizing the log-likelihood (ML method) ([Pinheiro et al., 2012](#)).

A possible biological effect of age on expression levels of individual genes was represented by fixed effects for each gene. A possible artificial effect of RNA quality (RIN value) on RT-qPCR results was modeled as a single fixed effect, allowed to vary randomly by each gene. This incorporation of RIN effects into the model was chosen, since the influence from RNA quality on RT-qPCR results should be small for short qPCR amplicons that we used in our study ([Fleige and Pfaffl, 2006](#)), and thus gene-dependent differences were expected to be minimal ([Fig. 1B–E](#) and [Supplementary Fig. S4](#)). But they should nevertheless be represented by the model ([Ho-Pun-Cheung, 2009](#); [Popova et al., 2008](#)), as RIN values of our PD brains were significantly higher than that of controls.

In addition, we have evaluated the influence of the confounders RIN value and age in isolation, by adjusting data for only one of these covariates ([Supplementary Table S4](#)). Comparison of these results under consideration of proportional change in variance (PCV) values allows dissecting which covariate has the strongest effects on the dependent variable.

2.5. General statistics

Data were analyzed and presented using R (www.r-project.com), Excel (Microsoft), Igor Pro (Wavemetrics), InStat and Prism (both

GraphPad). Data values are given as mean \pm standard error of the mean if not stated otherwise. Statistical differences for data in [Table 1](#), [Supplementary Table S3](#), and [Fig. 3A](#) were tested with Wilcoxon rank test. Data in [Table 2](#), [Supplementary Table S4](#), [Figs. 2 and 3B–E](#), and [Supplementary Fig. S2](#) were tested with Student *t* test (Welch-Test) after logarithmic transformation. Pairwise partial correlation coefficients in [Fig. 1A](#) were computed with the function *pcor* from the *ppcor* R package. The partial correlation factor is the Pearson correlation between 2 variables while controlling for all other variables. Pearson correlations in [Fig. 4](#) and [Table 3](#) were computed and tested for being different than zero after logarithmic transformation with standard functions of R. Correlation coefficients of a gene-pair for control and PD data were tested for significant differences by applying Steiger Z-test. *p*-values ≤ 0.01 were considered to be statistically significant and indicated by asterisk * ($p < 0.001$ and $p < 0.0001$ indicated as ** and ***, respectively).

3. Results

3.1. Characterization of human postmortem brain samples and evaluation of an RT-qPCR protocol for parallel mRNA and microRNA quantification

Eight controls and 5 PD postmortem brains were included in this study ([Table 1](#)). The RNA integrity (RIN) and donor age of PD brains were 7.28 ± 0.16 and 78.2 ± 1.3 year, respectively, which is significantly higher compared with the control cohort with 6.3 ± 0.1 and 69 ± 2 years, respectively (RIN, $p = 0.008$; age, $p = 0.016$; for 8 control and 5 PD brains). The relative amount of microRNA (miRNA) (% miRNA) was also lower in PD ($14.2\% \pm 1.6\%$) than in control brains ($24.9\% \pm 1.8\%$, $p = 0.032$). In addition, there was a

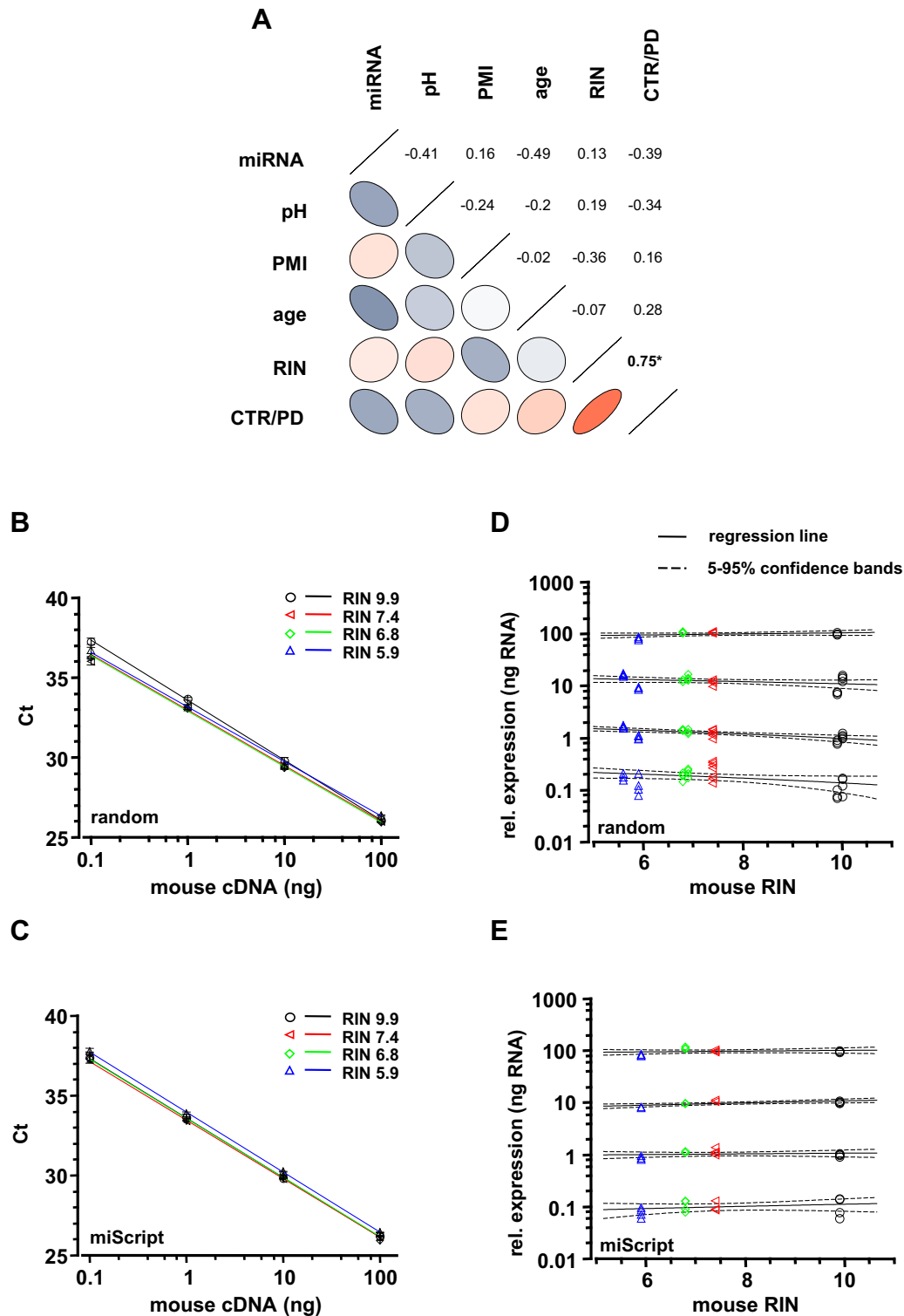


Fig. 1. Characterization of human postmortem brain samples and evaluation of RT-qPCR protocols for quantification of mRNA and miRNA. (A) Partial correlations between given parameters of brains analyzed in this study. Correlations between 2 parameters were controlled by the other 4 parameters in each calculation. Positive (red) or negative (blue) correlation given by orientation and color of ellipses, strength of correlation given by color intensity, and shape of ellipses, significant correlation indicated by asterisks. Note the strong significant correlation between RNA quality (given as RNA integrity number; RIN) and disease state (CTR vs. PD), due to significant difference of RIN values between control (CTR, $n = 8$) and PD ($n = 5$) brains (see also Table 1). Other correlations were not significant. (B–E) Sensitivity and reproducibility of both used RT-qPCR protocols (B/D: random primer protocol and C/E: miScript OligodT primer protocol) was independent of integrity-levels of RNA used as templates for cDNA synthesis (RIN range: 9.9–5.7 of mouse cDNA, covering the RIN-spectrum of the human samples of this study). (B/C) Note that sensitivity of qPCR assay (mLdh-2) is similar for all midbrain cDNA samples, each with 4 different RIN as templates ($p > 0.1$ in all comparisons; samples generated by thermal degradation of the same midbrain derived RNA for 0–72 minutes at 70 °C). (D/E) Results for RIN 9.9 from panels B and C (standard curve) were used for calculation of relative expression levels of mLdh-2 at different RIN values (range: 9.9–5.9). Regression lines with confidence bands show no significant dependence of gene expression levels from RIN values at all dilutions. Abbreviations: cDNA, complementary DNA; CTR, control; mRNA, messenger RNA; miRNA, microRNA; PD, Parkinson's disease; PMI, postmortem interval; RT-qPCR, quantitative real-time polymerase chain reaction.

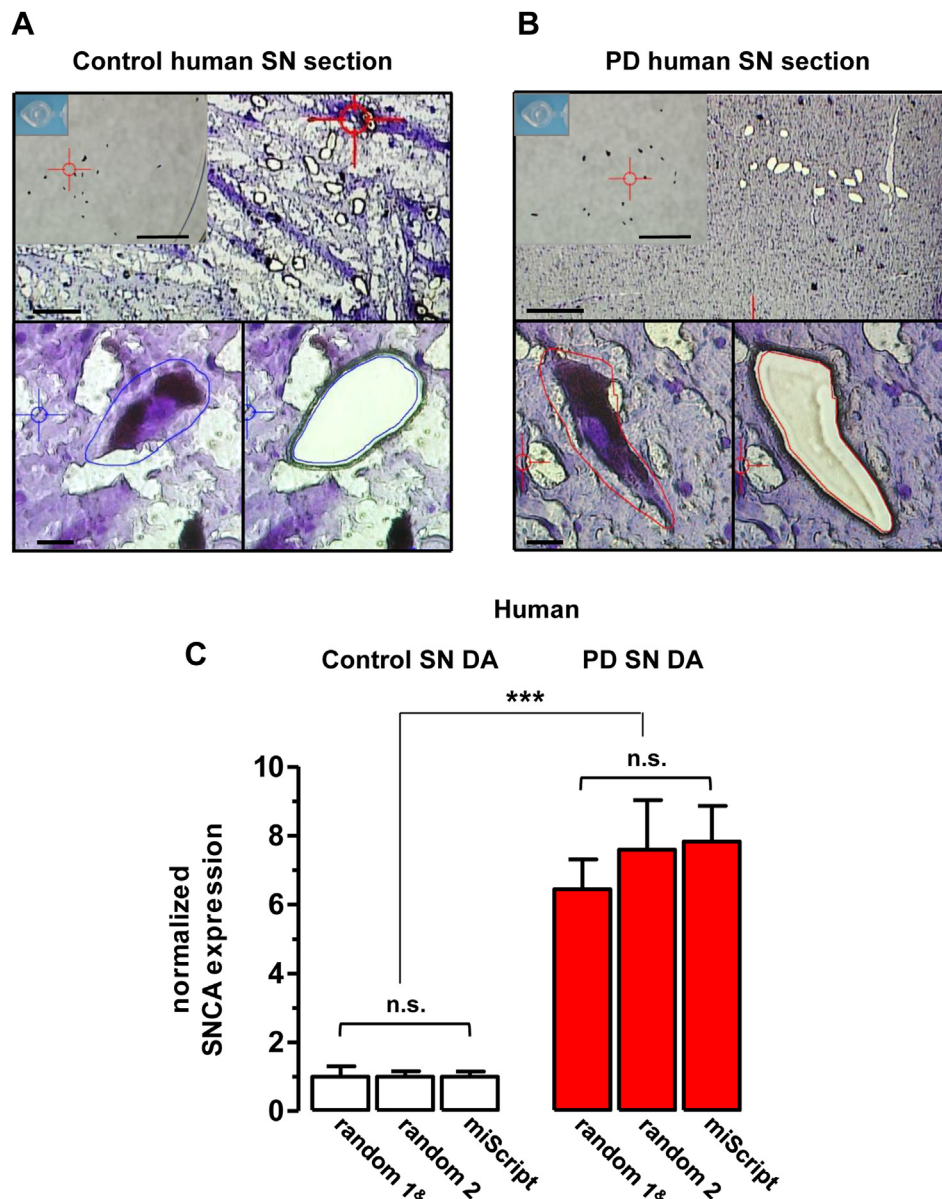


Fig. 2. UV-laser microdissection of individual, neuromelanin-positive substantia nigra dopamine neurons of human postmortem Parkinson's disease (PD) and control brains. (A–B) Upper row: overview of a control (A) and PD (B) horizontal midbrain kryo-section, containing the substantia nigra, after UV-laser microdissection (UV-LMD) of 15 individual, neuromelanin-positive neurons. Note the higher integrity of the PD tissue sections. Scale bars: 250 μ m. Inserts: photograph of the reaction tube cap for inspection of proper collection of all neurons before cell-lysis and reverse-transcription. Scale bars: 500 μ m. Lower row: individual substantia nigra dopamine neurons before (left) and after UV-LMD (right) from (A) control and (B) PD brains. Scale bars: 20 μ m. Note that all analyzed neuronal SN pools were qPCR-positive for tyrosine hydroxylase (TH). (C) Using the miScript RT-qPCR protocol, similar degrees of significantly elevated alpha-synuclein (SNCA) mRNA levels were detected in remaining SN DA neurons from PD brains compared with controls, as with our standard protocol (random 1, adapted from Grundemann et al., 2008 and random 2 for independent reproduction). Bar graphs (mean \pm SEM) show normalized SNCA expression levels of 3 individual SN DA sample sets from control brains (random 1, miScript 5: n = 5 brains; random 3: n = 8 brains) and PD brains (n = 5). For details see Table 2. Abbreviations: mRNA, messenger RNA; qPCR, quantitative polymerase chain reaction; SN DA, substantia nigra dopamine neurons; SEM, standard error of the mean.

significant correlation between disease state (control vs. PD) and RIN value, as evident from partial correlation coefficients (pcor, ppcor; Fig. 1A).

To evaluate and consider how differences in RNA quality affect results of our RT-qPCR experiments we applied 2 approaches. First, we designed a thermal degradation experiment to test whether our UV-LMD RT-qPCR protocols (random and miScript) display similar RT-qPCR results with similar amounts of RNA but with different RINs (Grundemann et al., 2008, 2011) (Fig. 1B–E). We generated cDNA from an identical RNA source (mouse midbrain) with distinct RINs generated by thermal degradation, either with our previously

published “random” protocol (using random hexamer primer) or with our new modified “miScript” protocol (using a combination of random and oligo-dT primers after polyadenylation of miRNAs). The RIN values ranged from 9.9 (fully intact RNA) to 5.9 (moderately degraded), covering the RIN spectrum of the human samples analyzed in this study (Table 1). To evaluate qPCR performance in dependence of RIN and cDNA amount, we prepared serial cDNA dilutions prior qPCR. Results for lactate dehydrogenase, mLdh-2 (and for other genes, data not shown) were similar for all samples independent from RIN or dilution factor as evident from both, threshold for cycle analysis values (Fig. 1B and C) and corresponding relative

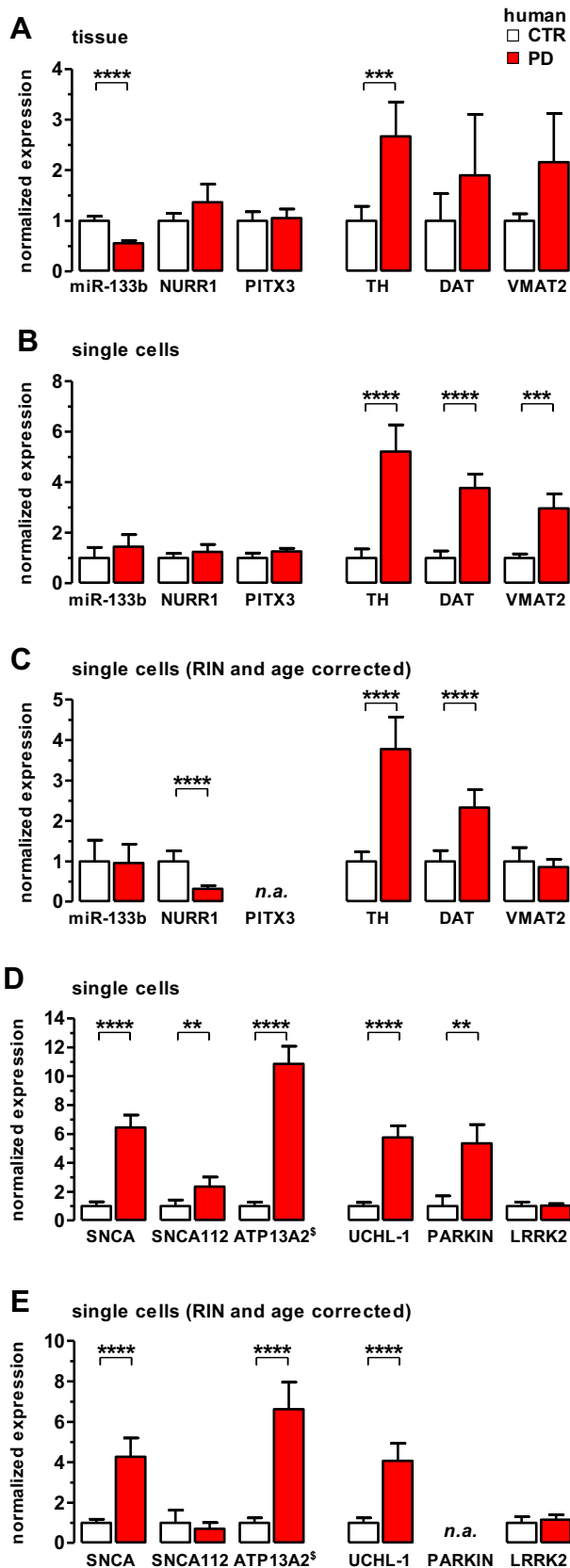


Fig. 3. Elevated mRNA levels of dopamine release genes and PARK genes in SNCA-overexpressing SN DA neurons in sporadic PD patients. (A) Levels of miR-133b and mRNAs for genes involved in DA neuron development and/or maintenance (NURR1, PITX3) and dopamine homeostasis (TH, DAT, VMAT2), determined via RT-qPCR at the level of midbrain tissue. Relative values, normalized to a geometrical mean of β -actin,

expression values, respectively (Fig. 1D and E); a prerequisite for RT-qPCR analysis of samples with significantly different RIN.

As evident from Fig. 1B–E (mouse midbrain) and Fig. 2C, (human SN DA neurons), our novel miScript RT-qPCR-approach allows quantification of mRNA independently of its integrity (for moderately degraded, RIN > 5.9) of small amounts of RNA (i.e., single cells), with a similar high sensitivity and reproducibility as our established protocol based on random hexamer primers (Grundemann et al., 2008). Quantification of SNCA mRNA for human neuromelanine- and TH-positive SN DA neurons using either the random hexamer protocol (experimental series random 1 and random 2) or the miScript approach resulted in similar results for control brains and PD brains analyzed in this study (Fig. 1F) and detected about 7-fold higher SNCA mRNA levels in surviving SN DA neurons in PD compared with controls, as we had previously described (experimental series random 1; Grundemann et al., 2008).

3.2. A linear mixed effects model allows data adjustment for possible age and RIN effects on differential gene expression data of PD and control SN DA neurons

To further take into account the possible effects of significantly different RINs and ages on gene expression comparison of SN DA neurons from PD and control brains, we optimized and applied a linear mixed effects model on our RT-qPCR data. (Koppelkamm et al., 2011; Popova et al., 2008). The model is described in detail in Section 2.

Model performance was assessed for TH expression data, available for all 5 sets of RT-qPCR data from this study. It was computed as change of the BIC compared with a model that considered only brain-dependent differences in Y-intercepts to account for inter-individual differences (in TH expression only) (Supplementary Fig. 1A) (Schwarz, 1978). The BIC value weights the goodness-of-fit against model complexity, with low values indicating better model performance. Based on this evaluation of model performance and the significantly different RIN and age values for PD and control brains, we decided to apply a 3-effects model, considering influence of disease state (CTR/PD), ages, and RINs for expression values of individual brains.

Our model was well applicable to all 5 UV-LMD RT-qPCR data sets and most analyzed genes (Supplementary Fig. 1B–F and Supplementary Table S2). Model results were not reliable for PARKIN and PITX3 data (data not shown), as the algorithm did not converge well (most likely because of low number of samples that gave positive RT-qPCR results).

3.3. Elevated mRNA levels of dopamine release genes and PARK genes but not of miR-133b in SN DA neurons from sporadic PD patients

After having established an RT-qPCR protocol for parallel miRNA and mRNA quantification, as well as the model for analyzing

ENO2, and TIF-1A. Note significantly lower expression of miR-133b and significantly higher levels of only TH in PD SN tissue compared with controls. (B–C) RT-qPCR analysis of genes as in (A), but at the cell-specific level of individual SN DA neurons, without (B) and after (C) adjustment of data for RIN and age effects. Note that miR-133b levels are not altered in SN DA neurons from PD compared with controls. (D and E) mRNA levels of PARK-genes in individual SN DA neurons, without (D) and after (E) model adjustment of data for RIN and age effects. n.a.: model-analysis not possible due to low numbers of samples with positive RT-qPCR results. Bar graphs represent normalized expression as mean \pm SEM. For details, see text. Abbreviations: DAT, dopamine transporter; mRNA, messenger RNA; PD, Parkinson's disease; RT-qPCR, quantitative real-time polymerase chain reaction; SEM, standard error of the mean; SN DA, substantia nigra dopamine neurons; TH, tyrosine hydroxylase; VMAT2, vesicular monoamine transporter 2.

Table 2

Relative mRNA levels in SN DA neurons from controls and PD brains, without and with mathematical adjustment for RIN and age. Relative mRNA levels (mean \pm SEM, determined via RT-qPCR) in individual SN DA neurons from PD brains compared with those from controls (given as pg-equivalents of standard SN cDNA per neuron), without and after adjustment for age- and RIN-influence

Experimental series	Gene	n		Relative expression (pg cDNA/cell)					RIN and age corrected relative expression (pg cDNA/cell)						
		CTR	PD	CTR	SEM	PD	SEM	p	PD/CTR	CTR	SEM	PD	SEM	p	PD/CTR
Random 1 ^a	ATP13A2	37	29	63.97	17.29	695.09	77.22	$<1 \times 10^{-6}$	10.87	85.93	21.48	569.26	115.06	$<1 \times 10^{-6}$	6.62
	SNCA	39	30	47.15	14.23	303.90	40.70	$<1 \times 10^{-6}$	6.45	58.87	15.43	259.66	58.88	$<1 \times 10^{-6}$	4.41
	TH	38	31	1139.08	451.35	11,641.23	1770.65	$<1 \times 10^{-6}$	10.22	1106.28	336.10	11,350.03	2524.68	$<1 \times 10^{-6}$	10.26
	UCLH1	39	32	132.80	34.11	765.77	106.04	$<1 \times 10^{-6}$	5.77	169.07	42.15	687.17	147.05	$<1 \times 10^{-6}$	4.06
Random 2	DAT	36	39	39.96	11.45	150.83	22.45	$<1 \times 10^{-6}$	3.77	52.66	14.18	122.89	23.15	4.16×10^{-5}	2.33
	TH	42	43	248.04	81.52	1849.62	359.46	$<1 \times 10^{-6}$	7.46	320.62	86.56	1307.27	276.91	$<1 \times 10^{-6}$	4.08
	VMAT2	15	33	23.22	3.82	69.00	13.12	2.54×10^{-4}	2.97	53.68	18.05	45.99	10.18	0.66	0.86
Random 3	PARKIN	8	10	875.30	622.13	4685.76	1137.45	1.06×10^{-3}	5.35	NA					
	SNCA	63	41	192.95	30.59	1465.18	278.79	$<1 \times 10^{-6}$	7.59	247.21	42.95	1098.55	235.20	$<1 \times 10^{-6}$	4.44
	SNCA112	16	18	37.31	16.23	87.92	24.92	5.64×10^{-3}	2.36	67.03	40.90	56.78	24.12	0.86	0.85
	TH	78	47	865.31	309.52	4514.34	918.54	$<1 \times 10^{-6}$	5.22	765.65	175.70	3003.64	634.08	$<1 \times 10^{-6}$	3.92
Random 4	LRRK2	26	30	5.84	1.64	6.05	0.84	0.14	1.04	6.30	1.88	7.23	1.57	0.29	1.15
	NURR1	28	34	36.25	6.74	44.92	10.95	1.00	1.24	69.59	17.40	22.28	5.73	2.35×10^{-5}	0.32
	TH	64	48	214.36	43.94	2818.29	734.13	$<1 \times 10^{-6}$	13.15	251.14	49.15	1985.90	455.40	$<1 \times 10^{-6}$	7.91
miScript 5	miR-133b	15	12	4.53	1.93	6.59	2.16	0.13	1.46	8.98	8.12	12.76	10.99	0.42	1.42
	PITX3	5	8	525.59	106.66	666.40	63.93	0.22	1.27	NA					
	SNCA	27	40	8.06	1.27	63.11	8.34	$<1 \times 10^{-6}$	7.83	22.89	7.80	52.04	11.58	1.02×10^{-3}	2.27
	TH	35	44	224.15	51.59	2426.00	324.47	$<1 \times 10^{-6}$	10.82	483.10	147.05	1977.50	415.15	$<1 \times 10^{-6}$	4.09

Differences were tested for significance with the Welch test after log-transformation (see Section 2).

Bold *p*-values indicate significant ($p < 0.05$) differences between CTR and PD.

Key: CTR, control; cDNA, complementary DNA; mRNA, messenger RNA; PD, Parkinson's disease; RIN, RNA integrity numbers; RT-qPCR, quantitative real-time polymerase chain reaction; SEM, standard error of the mean; SN DA, substantia nigra dopamine neurons; TH, tyrosine hydroxylase.

^a Data for TH, SNCA, and ATP13A2 are adapted from (Grundemann et al., 2008; Ramirez et al., 2006).

individual effects of human brain RIN, age, and disease state on RT-qPCR results, we used it for analysis of mRNA levels in individual, laser-microdissected SN DA neurons. For UV-LMD of individual neuromelanin-positive SN DA neurons, horizontal kryosections of the 8 controls and 5 PD brains (Table 1) were mounted on PEN membranes. We noted that the tissue integrity of all PD brains was appearing different to that of the control brains (Fig. 2A and B), PD tissue-integrity seemed to be better, presumably due to a reactive gliosis in the PD brain (Ahn et al., 2012; Członkowska and Kurkowska-Jastrzębska, 2011). Only neuromelanin-positive neurons with visible nuclei and intact morphology within the SN were laser-microdissected (Fig. 2A and B) and lysed for subsequent RT-qPCR analysis.

We analyzed the expression of several dopamine maintenance and release genes (SNCA, TH, DAT, VMAT2, NURR1, PITX3) and PARK genes (SNCA, ATP13A2, UCLH1, PARKIN, LRRK2) as well as the microRNA miR-133b.

We evaluated miR-133b levels from PD and control midbrain tissue, as well as from individual SN DA neurons, since a previous study reported reduced amounts of miR-133b in PD, associated with increased amounts of DA maintenance and release genes in PD brains at the midbrain tissue level (Kim et al., 2007). We confirmed a reduction of miR-133b in PD at the midbrain tissue level (Fig. 3A and Supplementary Table S3; note that total % miRNA levels were also significantly lower in PD brain tissue, see Table 1). However, at the single cell level, we detected no differences in miR-133b levels in SN DA neurons between PD and controls (Fig. 3B and C, Supplementary Fig. S2 and Table 2). These results emphasize the importance of cell-specificity when comparing gene expression of complex tissues with variations in the number of target cells because of disease state, as it is the case for SN DA neurons in midbrain tissue in PD compared with controls.

In accordance with unaltered miR-133b levels, we detected no changes in PITX3 and NURR1 levels in PD compared with controls at both, tissue and SN DA specific level (Fig. 3A and B, Supplementary Fig. S2, Table 2, and Supplementary Table S3 and S4). PITX3 and NURR1 expression was suggested to be regulated by miR-133b and

is important for specification and maintenance of the SN DA neuronal phenotype (Kim et al., 2007; Volpicelli et al., 2012). Mathematical adjustment of cell-specific data for age and RIN effects of NURR1 expression (3-effects-model) suggests a down-regulation of NURR1 in PD (Fig. 3C, and Table 2). Moreover, the model suggests a rather complex change where disease state (PD) reduced NURR1 expression, while age increased it (Supplementary Figs. S2 and S3, and Supplementary Table S4). Note that marginal R^2 is very low, and the PCV is about 70% (Supplementary Table S2). This might imply that the model has only little explanatory power for NURR1, as the variance at the cell level is much larger than inter-individual variance between brains. Since the model does only account for inter-individual differences (RIN, age, CTR/PD) but not expression differences between cells of the same individual, a prominent variance at the cell level leads to small marginal R^2 values. For NURR1 most of the inter-individual variance captured by the model is explained by PD and age (see $PCV_{CTR/PD}$, PCV_{+age} in Supplementary Table S2), not by random intercept effects. PITX3 data could not be adjusted for age and RIN, since the algorithm did not converge to an optimum, due to low number of samples with positive RT-qPCR results.

In contrast to miR-133b, PITX3, and NURR1, mRNAs for tyrosine hydroxylase (TH), the rate limiting enzyme for dopamine synthesis, as well as for SNCA were dramatically increased in SN DA neurons from PD patients compared with controls (as we had previously reported Grundemann et al., 2008), reproducible in all experimental series (from consecutive sections of individual brains; Fig. 2C, Fig. 3A–C, Table 2, and Supplementary Fig. S2). Also, expression levels of the plasma membrane dopamine transporter (DAT), important for axonal and somatodendritic dopamine re-uptake as well as for the vesicular monoamine transporter 2 (VMAT2) were significantly increased (Fig. 3B, Table 2, and Supplementary Fig. S2). Interestingly, increased expression of VMAT2 in PD is not preserved after adjustment for RIN and age effects (Fig. 3C and Table 2). This is based on the fact, that VMAT2 expression levels of different brains are well represented by a linear age dependence (Supplementary Figs. S2 and S3, value of PCV_{+age} in

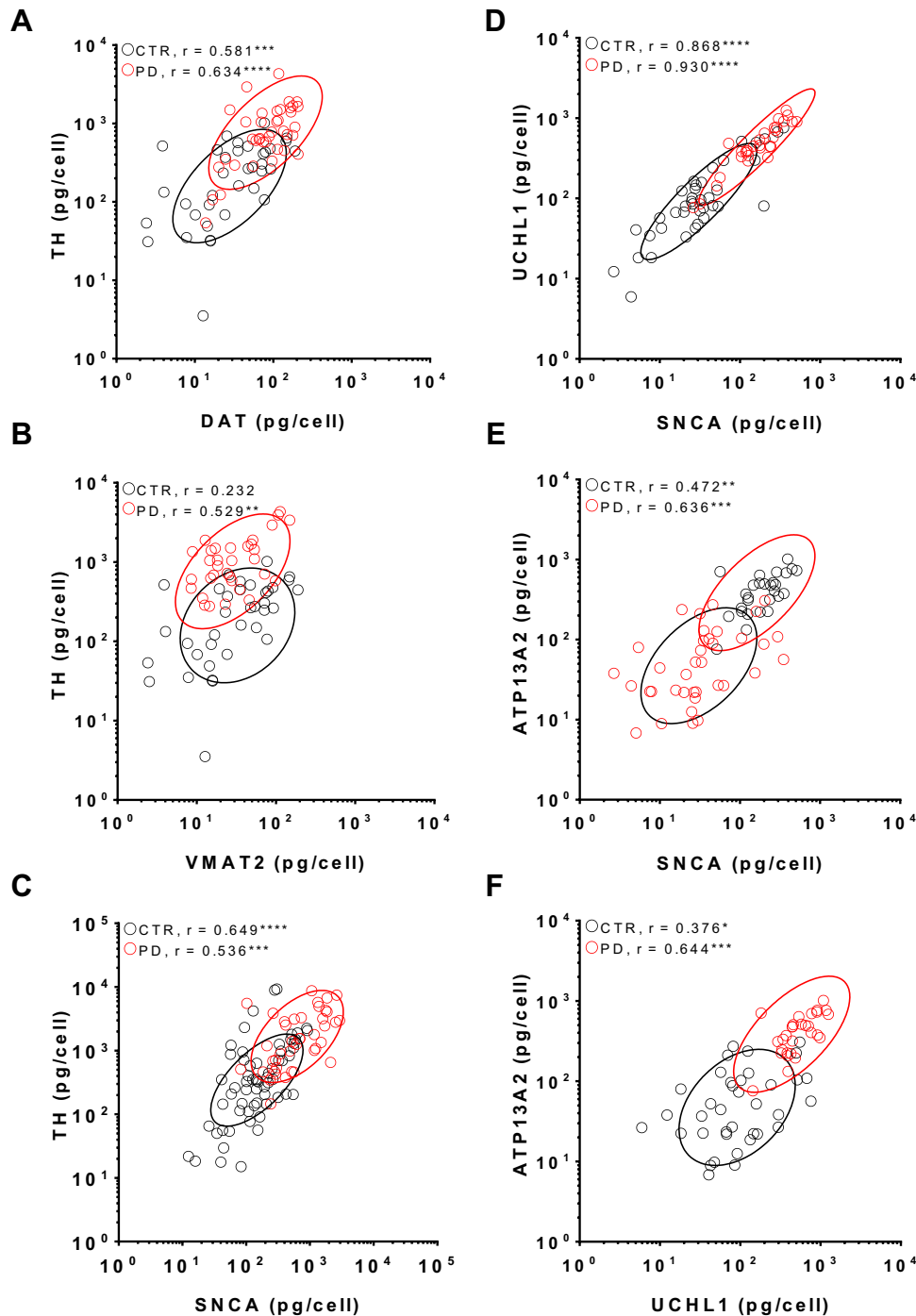


Fig. 4. Cell-specific, positive correlations of elevated mRNA levels for dopamine synthesis and PARK-genes in human SN DA neurons. (A–F) Individual scatter plots of relative mRNA levels (after model-adjustment) for controls (CTR, white circles) and PD brains (red circles) of selected gene-pairs (logarithmic scales). Ellipses are drawn at the 75% confidence level for control (black) and PD (red). Elongated ellipses indicate strong correlation. R-values give Pearson correlation coefficients. Significant correlations are indicated by asterisks (* $p < 0.01$, ** $p < 0.001$, *** $p < 0.0001$). Differences in correlations of PD and control data were identified by Steiger Z-test and marked by asterisks. For detailed analysis of all gene-pairs see Table 3. Abbreviations: mRNA, messenger RNA; PD, Parkinson's disease; SN DA, substantia nigra dopamine neurons.

Supplementary Table S2 and S4: note no difference in VMAT2 expressions between PD and controls, after adjusting only for age effects). These findings further highlight the importance of the 3-effects-model analysis of the RT-qPCR data, as our human PD and control samples were not perfectly age matched.

As expression levels of the SNCA splice variant SNCA112 have been associated with higher risk for PD (McCarthy et al., 2011), we also specifically analyzed the mRNA levels of SNCA112. As

expected, SNCA112 was expressed at significantly lower levels in human control SN DA neurons compared with the unspecific SNCA assay, which detects SNCA140 as well as SNCA112 (~5%, $p < 0.001$). A PD-related increased expression of SNCA112 is however not detected after correction for age and RIN (Fig. 3D–E, Table 2, and Supplementary Fig. S2). The elevated SNCA112 expression in the PD cohort is, according to the model analysis, rather associated with age differences (Supplementary Table S2 and S4; note no

Table 3

Cell-specific positive correlations of elevated mRNA levels for dopamine synthesis and PARK-genes in human SN DA neurons

Experimental series	Gene pairs	CTR			PD			All		Correlations comparison (CTR and PD)
		n	r	p	n	r	p	r	p	
Random 1 ^a	ATP13A2-SNCA	37	0.472	0.003	28	0.636	2.72 × 10⁻⁴	0.756	<1 × 10⁻⁶	0.36
	ATP13A2-TH	36	0.173	0.31	29	0.493	0.007	0.693	<1 × 10⁻⁶	0.16
	SNCA-TH	38	0.434	0.006	29	0.637	2.00 × 10⁻⁴	0.734	<1 × 10⁻⁶	0.27
	UCHL1-ATP13A2	37	0.376	0.02	29	0.644	1.63 × 10⁻⁴	0.730	<1 × 10⁻⁶	0.16
	UCHL1-SNCA	39	0.868	<1 × 10⁻⁶	30	0.930	<1 × 10⁻⁶	0.932	0	0.19
	UCHL1-TH	38	0.480	0.002	31	0.661	5.13 × 10⁻⁵	0.756	<1 × 10⁻⁶	0.28
Random 2	TH-DAT	36	0.581	2.06 × 10⁻⁴	39	0.634	1.50 × 10⁻⁵	0.705	<1 × 10⁻⁶	0.73
	VMAT2-DAT	14	0.289	0.32	31	0.301	0.10	0.191	0.21	0.97
	VMAT2-TH	15	0.232	0.40	33	0.529	0.002	0.314	0.03	0.30
Random 3	SNCA112-TH	16	0.468	0.07	18	0.144	0.57	0.330	0.06	0.34
	SNCA-SNCA112	15	0.247	0.38	18	0.560	0.016	0.326	0.06	0.33
	SNCA-TH	63	0.649	<1 × 10⁻⁶	41	0.536	3.09 × 10⁻⁴	0.721	0	0.40
Random 4	LRRK2-TH	26	0.585	0.002	30	-0.152	0.42	0.275	0.04	0.004
	NURR1-LRRK2	9	-0.400	0.29	21	0.387	0.08	0.185	0.33	0.08
	NURR1-TH	28	0.324	0.09	34	-0.150	0.40	-0.379	0.002	0.07
miScript 5	miR-133b-SNCA	11	0.319	0.34	11	0.214	0.53	0.196	0.38	0.82
	miR-133b-TH	15	0.514	0.05	12	-0.594	0.042	0.150	0.46	0.005
	SNCA-TH	27	0.320	0.10	40	0.622	1.82 × 10⁻⁵	0.514	<1 × 10⁻⁶	0.13

Cell-specific correlation and regression analysis of mRNA levels of gene-pairs for SN DA neurons from PD brains compared with controls. Correlation coefficients were computed on log-transformed data.

SN DA samples (n) were derived from 5 PD brains for all experimental series, and from 5 control brains for random series 1, 2, and miScript series 5, and 8 control brains for series 3 and 4.

Bold *p*-values indicate significant (*p* < 0.05) correlations or differences of correlations between PD and control. For details of analysis, see Section 2.

Key: CTR, control; mRNA, messenger RNA; PD, Parkinson's disease; SN DA, substantia nigra dopamine neurons; TH, tyrosine hydroxylase.

^a Data for TH, SNCA, and ATP13A2 analysis adapted from (Grundemann et al., 2008; Ramirez et al., 2006).

difference in SNCA112 expressions between PD and controls, after adjusting them for age-effects. Also note that the large PCV_{CTR/PD} is a consequence of significant older ages of PD brains).

As not only SNCA expression is dramatically elevated in SN DA neurons from PD but also the expression of the p-type ATPase ATP13A2 (PARK9; Ramirez et al., 2006 as well as Fig. 3D–E, Table 2, and Supplementary Fig. S2) we determined mRNA levels for 3 further PARK genes: UCHL1, PARKIN, and LRRK2. While for LRRK2 (PARK8) we detected no change in mRNA level in PD samples compared with controls (Fig. 3D–E, Table 2, and Supplementary Fig. S2), for UCHL1 (PARK5) and PARKIN (PARK2) we detected about 5-fold higher mRNA levels in PD (note that only 8 of 78 TH-positive control samples from 3 brains and 10 of 47 TH-positive PD samples from 4 brains gave RT-qPCR results for PARKIN; this low brain and sample number prevented the fitting algorithm to converge to a reliable result—n.a.).

3.4. SNCA mRNA levels correlate with transcripts for dopamine synthesis in SN DA neurons from PD patients

The increased levels of mRNA for genes involved in dopamine synthesis and transport as well as for PARK genes suggest an altered functional state of SN DA neurons from PD patients. To gain further insights into concerted increased gene expression in surviving SN DA neurons with confirmed elevated mRNA levels for both TH and SNCA, we performed a correlation analysis at the level of SN DA neurons for all analyzed genes within the same experimental series. A possible significant correlation of mRNA expression for 2 genes was tested after logarithmic transformation by Pearson correlation coefficient (all correlation data are given in Table 3, while Fig. 4 highlights selected correlations).

We detected a significant correlation between TH and DAT expression, involved in dopamine synthesis and reuptake, thus determining (in interplay with VMAT2) the free cytosolic dopamine concentration (Fig. 4A and B and Table 3: controls *r* = 0.58, *p* < 0.001;

PD: *r* = 0.63, *p* < 0.0001). In accordance with the predominantly age-related increase in VMAT2 mRNA, identified by our model analysis, VMAT2 mRNA level were only weakly correlated to TH, only in PD (Table 3). Our finding would be in line with a compensatory genetic program in PD, leading to a concerted upregulation of dopamine synthesis, packaging, and release capacity. This interpretation is further supported by the robust strong positive correlation between TH-mRNA and SNCA-mRNA detected in 3 independent experiments (Fig. 4C and Table 3, correlation factors for experimental series random 1: controls *r* = 0.43, *p* = 0.006; PD *r* = 0.64, *p* < 0.001; random 3: controls *r* = 0.65, *p* < 0.001; PD *r* = 0.54, *p* < 0.001; and miScript 5: controls *r* = 0.32, *p* = 0.1; PD *r* = 0.62, *p* < 0.001).

While in our data no correlation between miR-133b levels and SNCA expression was detectable (Table 3), a negatively correlated association of miR-133b to TH expression was weakly significant for PD samples (Table 3). In light of this finding, it is tempting to speculate that in PD miR-133b is involved in a genetic program that is able to decrease TH expression, and thus dopamine-synthesis, but note the low sample numbers with positive qPCR for miR-133b results, which inevitably leads to low power of the statistical tests.

3.5. SNCA (PARK1/4) expression correlates with transcripts for ATP13A2 (PARK9) and UCHL1 (PARK5) in SN DA neurons from PD brains

Given the crucial role of SNCA levels for SN DA degeneration in PD, and it is still unknown relation to other confirmed PARK genes, we probed for possible orchestrated increased gene expression of SNCA and the other PARK genes, for which we detected significantly higher mRNA levels in SN DA neurons of PD patients (UCHL1 and ATP13A2; Fig. 4E and Table 3). We detected the strongest, highly significant, positive pair-wise correlation for SNCA and UCHL1 mRNA levels in SN DA neurons from control as well as from PD brains (Fig. 4D). We also found a strong positive significant

correlation between SNCA and ATP13A2 (PARK9), and consequently, also for UCHL1 and ATP13A2 in SN DA neurons from controls as well as from PD (Fig. 4E and F). These data indicate strongly coupled gene expression of SNCA, UCHL1, and ATP13A2, already present in SN DA neurons under control conditions, showing a concerted upregulation in PD.

4. Discussion

To address the complex cellular transcriptome in which different RNA species interact in a network (Salmena et al., 2011), we extended our mRNA quantification method for human SN DA neurons to allow unbiased parallel quantification of mRNAs and miRNAs from the same UV-LMD sample via RT-qPCR. Variable RNA integrities (RIN) are unavoidable across human postmortem samples with individual, non-standardized premortal and postmortal history. RIN variability can significantly bias microarray and RT-qPCR gene expression results (Schwarz, 1978), a possible explanation for differences in results of various expression-profiling studies (Bustin et al., 2010; Grundemann et al., 2008; Vermeulen et al., 2011). However, both, our newly developed miScript protocol and our previously described random primer based RT-qPCR protocol performed equally well for samples with differentially degraded mouse RNA within the RIN-range of the human brains, analyzed here (Fig. 1B–E).

To further dissect possible confounding contributions of the covariables age and RIN to the observed expression changes for the individual tested genes in SN DA neurons from PD brains, compared with that of controls, we developed a linear-mixed 3-effects model (Snijders and Bosker, 2011). Bias in the analysis and interpretation of expression data because of covariables can be reduced by optimal matching in the study design and stratification (Consonni et al., 1997). However, stratification needs large sample numbers on each hierarchical level with possible confounders (i.e. brains in our case). This is usually particularly difficult to achieve for limited human samples, such as human postmortem brain samples (McNamee, 2005). The brains provided for this study were not perfectly matched in regard to their RNA quality (RIN value) and the age of donors. Since both quantities have to be considered as relevant confounders, their influence on detected gene expression values had to be estimated. We have statistically reanalyzed data with our linear-mixed 3-effects model, a method based on mathematical regression (Consonni et al., 1997; McNamee, 2005). All model details, the algorithm, and its evaluation are discussed in detail in the supplement.

With this novel methodological approach, we detected orchestrated, positively correlated elevated expression of dopamine homeostasis genes (TH, DAT, VMAT2, SNCA) as well as PARK-genes (SNCA, ATP13A2, UCHL1, PARKIN) in remaining human SN DA neurons from PD brains compared with those of controls. These changes were not associated with reduced levels of miR-133b, as recently suggested (Kim et al., 2007). However, our correlative expression data do not give direct proof or provide insight into the mechanisms of gene interaction, and differences in mRNA abundances might not always simply be translated into different abundances of functional proteins (Tang et al., 2011; Tobin, et al., 2009).

For most genes, for which we detected significantly higher mRNA levels in SN DA neurons from PD compared with controls, the model also predicted predominantly disease-associated increases, not caused by age or RIN (TH, SNCA, DAT, PARKIN, UCHL1, ATP13A2). For VMAT2 and SNCA112 modeling suggested an age-dependent change with no or only moderate effects of PD. For NURR1 the model suggested a PD related reduction of expression in SN DA neurons, which was compensated by an age-related increase in mRNA levels. Although it is tempting to speculate that age-

dependent changes in gene expression could be causative for PD, it has to be emphasized that the model results are in general based on a low number of brains giving more or less large inter-individual differences in covariables and RT-qPCR results, thus such conclusions certainly need further investigation. However, the model reliably allows us to exclude relevant bias of our gene expression data by differences in RNA quality (compare Supplementary Table S2 and S4), a prerequisite when performing RT-qPCR analysis for samples with significantly different RIN, as it was the case for our human brain samples.

4.1. Cellular specificity is critical for detecting concerted changes of gene expression in SN DA neurons in PD

Cell-specific gene expression analysis is the desired standard for quantification of individual mRNA or miRNA species, and as shown here, to identify cell-specific concerted correlations of gene expression at the RNA level (Ransdell et al., 2010; Stahlberg et al., 2011; Tang et al., 2011; Tobin et al., 2009). Cell specificity is important for understanding the transcriptional networks that define distinct cellular phenotypes (Schulz et al., 2007; Tobin et al., 2009), as well as to identify cell-specific perturbations in disease. Studies of genetic interactions and responses to alpha-synuclein overexpression and its toxicity have been carried out in model organisms (Auluck et al., 2010), reporting upregulations of several genes in response to alpha-synuclein overexpression, however, up to now only at the tissue level (Scherzer et al., 2003; Vartiainen et al., 2006).

However, in the pars compacta of human SN, most neurons are dopaminergic and in PD motor symptoms manifest when approximately 70% of these DA neurons are already lost (Damier et al., 1999). Thus, midbrain tissue in PD and control brains is composed of a significantly different mix of DA and non-DA (e.g., glia, GABA) cells. In addition to the dramatic reduction of DA neurons in midbrain tissue in PD, analysis at the tissue level is additionally confounded by altered numbers and functional states of non-neuronal cells like microglia, astrocytes, and local T-cells (Hirsch and Hunot, 2009; Schwarz, 1978). Thus, cell-specificity is crucial when comparing gene expression changes in the SN in PD and control states. As we show here, the problem of detected tissue-based, artificial differences in gene expression between PD and control midbrains also applies to qPCR-based quantification of miRNAs, and might explain recent controversial findings from tissue-based studies (de Cremoux et al., 2011; Jung et al., 2010; Kim et al., 2007; Opitz et al., 2010; Schwarz, 1978).

For miR-133b, DAT, and VMAT2 we obtained different results between tissue level-based and cell-specific RNA quantification. Only the most prominent elevation of TH in SN DA neurons from PD brains compared with controls was still detectable at the midbrain tissue level. Restricting the analysis to the tissue level would miss gene expression changes of DAT and VMAT2, as it might have occurred in various SN tissue-based expression studies (Lesnick et al., 2007; Mandel et al., 2005; Moran et al., 2006; Zhang et al., 2005). This indicates that extrapolations of expression results based on whole SN midbrain tissue to the individual SN DA neuron, as recently done for miR-133b (Kim et al., 2007), (Junn and Mouradian, 2012; for critical discussion), might be misleading (Fig. 3). Similar as Kim et al. (2007), we detected significantly reduced amounts of miR-133b in whole SN midbrain tissue from PD patients compared with controls. However, at the cell-specific level of individual neuromelanine-positive SN DA neurons, miR-133b expression was not altered in PD compared with control, in accordance with recent similar notes (Heyer et al., 2012; Minones-Moyano et al., 2011; Sonntag, 2010). Accordingly, variants in miR-133 and PITX3 genes in PD patients and controls seem not to contribute to the risk for PD (de Mena et al., 2010).

4.2. Concerted elevated mRNA levels of dopamine homeostasis and PARK genes in SNCA-overexpressing SN DA neurons from PD brains

In individual SN DA neurons, we detected significantly higher mRNA levels of VMAT2 < DAT < SNCA112 < UCHL1 < PARKIN in our PD brains, in addition to those of TH, SNCA, and ATP13A2 as previously described (Grundemann et al., 2008; Ramirez et al., 2006) (Fig. 3 and Table 2).

Our findings for TH, DAT, SNCA, UCHL1, and ATP13A2 in PD brains are in contrast to another SN DA-specific UV-LMD based RT-qPCR study (Simunovic et al., 2009), most likely because of methodological differences (different SN DA sampling sizes, pre-amplification, and normalization to housekeeping genes).

PARKIN is involved in catabolic autophagy and mitophagy, essential for organelle quality control and global starving response (Youle and Narendra, 2011) that might be particularly important in PD, as a protective response to an increased load of neurotoxic alpha-synuclein (Kamp et al., 2010; Mszczynska et al., 2007).

4.3. Positive correlation of mRNA levels for TH-DAT-VMAT2 in SNCA-overexpressing SN DA neurons in PD

We show that SNCA mRNA abundance is positively correlated with that of TH (the rate-limiting enzyme for dopamine synthesis) in SN DA neurons from controls as well as from PD brains. TH mRNA expression was further correlated with DAT mRNA, which codes for the dopamine uptake transporter and only in PD patients positively correlated with the mRNA of the vesicular monoamine transporter VMAT2. The increased expression of TH, DAT, and VMAT2 together with SNCA in SN DA neurons in the PD brains is in accordance with increased dopamine-release machinery because of SN DA neuron loss in PD or older age (Li et al., 2010). Our findings might indicate a larger transcriptional or mRNA stability network (Reddy et al., 2011), enabling surviving SN DA neurons in advanced PD to synthesize (TH), package (VMAT2), release (SNCA), and re-uptake (DAT) dopamine (Zhou et al., 2011). For example, TH, DAT, and VMAT2 expression are all regulated by BDNF signaling (Boger et al., 2011; Fukuchi et al., 2010; Ziebell et al., 2010). Increased expression of SNCA, possibly mediated by altered SNCA-methylation (Jowaed et al., 2010) or reduced miRNA activity (Jung et al., 2010; Wang et al., 2008) might be a trigger for SN DA degeneration and PD but also be embedded in this compensatory response of the dopamine system (Lundblad et al., 2012). Of 4 isoforms of SNCA (generated by alternative splicing of exons 3 and 5: Venda et al., 2010), the SNCA112 splice variant (no exon 5) was found in particular in brains from patients with Lewy body disease and its levels were upregulated in cell culture by the PD toxin MPP⁺ (Kalivendi et al., 2009; Venda et al., 2010). Therefore, we specifically analyzed mRNA levels of SNCA112 in SN DA neurons from PD and control brains and detected a 2.4-fold increase in SNCA112 mRNA in our PD brains. Although, our model suggested that this increase was mainly related to age, there was a significant correlation of SNCA112 mRNA levels with that of the unspecific SNCA assay (detecting full length SNCA140 + 112) only in PD (Table 3). This might support the idea of PD-associated alternative SNCA splicing as a protective strategy during global SNCA overexpression (McCarthy et al., 2011; McLean et al., 2011; Venda et al., 2010).

4.4. Positive correlation of mRNA levels for UCHL1 and ATP13A2 in SNCA-overexpressing SN DA neurons in PD

In addition to facilitating dopamine release, increased levels of alpha-synuclein are also expected to increase the toxic protein load for proteasomal and lysosomal protein degradation (Auluck et al., 2010). A prominent modifier gene for alpha-synuclein

overexpression-induced toxicity is ATP13A2 (PARK9), a lysosomal ATPase of still unknown function (Gitler et al., 2009; Radi et al., 2011). The PD-mutated form of ATP13A2 sensitizes cells to ER-stress induced cell death (Ugolino et al., 2011). ATP13A2 (PARK9) has been identified as a suppressor of alpha-synuclein toxicity (Gitler et al., 2009). Accordingly, ATP13A2 mRNA levels are increased in remaining SN DA neurons from sporadic PD patients compared with controls (Ramirez et al., 2006).

Our study demonstrates that in SN DA neurons of controls as well as PD, SNCA, and ATP13A2 expression is positively correlated, indicating that ATP13A2 expression might be scaled-up in PD in response to a toxically increased alpha-synuclein load. We detected an even stronger significant correlation between SNCA mRNA expression and UCHL1 (PARK5), and accordingly also between ATP13A2 and UCHL1 in SN DA neurons from controls and PD. UCHL1 is an ubiquitin hydrolase that is a component of the ubiquitin-proteasome pathway, and has been identified together with alpha-synuclein in Lewy bodies (Yasuda et al., 2009). Increased striatal UCHL1 expression is also present in a mouse overexpressing wild-type SNCA (Prasad et al., 2011) and reduced UCHL1 levels reduce neuronal survival (Lombardino et al., 2005). These findings indicate a concerted regulation of these PARK-genes in SN DA neurons in PD, as a protective response to increased proteasomal and lysosomal and/or autophagosomal demands. The finding that LRRK2 (PARK8) mRNA levels were not altered in remaining DA neurons from PD brains is in accordance with a study showing that pathogenic LRRK2 mutations do not alter gene expression in human brain tissue (Devine et al., 2011a). Increased expression of wild-type LRRK2 accelerates alpha-synuclein-induced neurodegeneration and is thus not expected as an allostatic survival mechanism of SN DA neurons in PD (Caguci, 2003; Lin et al., 2009).

In summary, we identified a concerted upregulation of selected dopamine homeostasis and PARK genes in surviving, alpha-synuclein and TH overexpressing human SN DA neurons in sporadic PD, apparently not orchestrated by altered miR-133b levels. This correlated increase of mRNAs in SN DA neurons from sporadic PD patients suggests a coupling of disease-triggering alpha-synuclein expression in SN DA neurons with transcriptional compensatory programs. This might favor a functional compensation network in SN DA neurons to increase their dopamine release (TH, DAT, VMAT2, and SNCA) and, on the other hand, to stimulate proteasomal (UCHL1, PARKIN) as well as lysosomal (ATP13A2) function to counteract alpha-synuclein toxicity. This compensatory network might be orchestrated at the level of, for example, stress-induced specific transcription factors, jointly regulating these genes. However, further studies (e.g., promoter-analyses) are needed to test this hypothesis.

Global gene expression studies addressed gene networks of transcriptional dysregulation for mammalian DA neurons in PD (Elstner et al., 2011; Greene, 2011; Moran and Graeber, 2008). Expression profiling studies and complementary genetic screens resulted in largely nonoverlapping gene lists (Schwarz, 1978), which are integrated in novel bioinformatics tools such as ResponseNet (Yeger-Lotem et al., 2009). Future cell-specific gene expression data need to extend and combine all these approaches, ideally with parallel analysis of respective genetic risk factors to define whether mRNA level correlations, as well as certain micro-RNA expression patterns constitute molecular signatures of surviving SN DA neurons in PD patients (Palm et al., 2012), and thus offer molecularly defined targets for protecting DA neurons.

Disclosure statement

Authors disclose any actual or potential conflicts of interest including any financial, personal or other relationships with other

people or organizations within 3 years of beginning the work submitted. All experiments were in accordance with and approved by the ethic commission of Ulm University, Germany (247/10-UBB/bal). All animal procedures were approved by the Regierungspräsidentium Tübingen, Germany.

Acknowledgements

This work was supported by the National Genome Research Network program from the Federal Ministry of Education and Research (01GS08134), the Gemeinnützige Hertiestiftung, the German Research Foundation (DFG, SFB479, LI1745/1-1), and the Royal Society, UK. Jan Gründemann is supported by an EMBO long-term fellowship and Marie Curie Actions. Birgit Liss is supported by the Alfried Krupp prize.

The authors are particularly grateful to the brain donors and the support by the German BrainNet (GA28). They thank Gaby Schneider for critical discussion, Dietmar Thal for providing additional human brain samples, and Leica Microsystems for providing the LMD6000. The authors are responsible for the content of this publication. Falk Schlaudraff and Jan Gründemann contributed to experiments and data analysis. Michael Fauler contributed to model development, detailed data analysis, and statistics. Elena Dragicevic contributed to data analysis and data presentation. John Hardy contributed to critical data discussion, and Birgit Liss designed study and wrote the manuscript.

Appendix A. Supplementary data

Supplementary data associated with this article can be found, in the online version, at <http://dx.doi.org/10.1016/j.neurobiolaging.2014.03.016>.

References

- Ahn, T.B., Langston, J.W., Achi, V.R., Dickson, D.W., 2012. Relationship of neighboring tissue and gliosis to α -synuclein pathology in a fetal transplant for Parkinson's disease. *Am. J. Neurodegener. Dis.* 1, 49–59.
- Auluck, P.K., Caraveo, G., Lindquist, S., 2010. alpha-Synuclein: membrane interactions and toxicity in Parkinson's disease. *Annu. Rev. Cell Dev. Biol.* 26, 211–233. <http://dx.doi.org/10.1146/annurev.cellbio.042308.113313>.
- Boger, H.A., Mannangatti, P., Samuvel, D.J., Saylor, A.J., Bender, T.S., McGinty, J.F., Fortress, A.M., Zaman, V., Huang, P., Middaugh, L.D., Randall, P.K., Jayanthi, L.D., Rohrer, B., Helke, K.L., Granholm, A.C., Ramamoorthy, S., 2011. Effects of brain-derived neurotrophic factor on dopaminergic function and motor behavior during aging. *Genes Brain Behav.* 10, 186–198. <http://dx.doi.org/10.1111/j.1601-183X.2010.00654.x>.
- Bustin, S.A., Beaulieu, J.F., Huggett, J., Jaggi, R., Kibenge, F.S., Olsvik, P.A., Penning, L.C., Toegel, S., 2010. MIQE precis: practical implementation of minimum standard guidelines for fluorescence-based quantitative real-time PCR experiments. *BMC Mol. Biol.* 11, 74. <http://dx.doi.org/10.1186/1471-2199-11-74>.
- Cagaci, D.G., 2003. *Sensitivity and Uncertainty Analysis – Volume 1: Theory*. Chapman&Hall/CRC Press, New York.
- Consonni, D., Bertazzi, B.A., Zocchetti, C., 1997. Why and how to control for age in occupational epidemiology. *Occup. Environ. Med.* 54, 772–776. <http://dx.doi.org/10.1136/oem.54.11.772>.
- Członkowska, A., Kurkowska-Jastrzebska, I., 2011. Inflammation and gliosis in neurological diseases—clinical implications. *J. Neuroimmunol.* 231, 78–85.
- Damier, P., Hirsch, E.C., Agid, Y., Graybiel, A.M., 1999. The substantia nigra of the human brain. II. Patterns of loss of dopamine-containing neurons in Parkinson's disease. *Brain* 122 (Pt 8), 1437–1448.
- de Cremoux, P., Valet, F., Gentien, D., Lehmann-Che, J., Scott, V., Tran-Perennou, C., Barbaroux, C., Servant, N., Vacher, S., Sigal-Zafrani, B., Mathieu, M.C., Bertheau, P., Guinebreteiere, J.M., Asselain, B., Marty, M., Spyrtas, F., 2011. Importance of pre-analytical steps for transcriptome and RT-qPCR analyses in the context of the phase II randomised multicentre trial REMAGUS02 of neoadjuvant chemotherapy in breast cancer patients. *BMC Cancer* 11, 215. <http://dx.doi.org/10.1186/1471-2407-11-215>.
- de Mena, L., Coto, E., Cardo, L.F., Diaz, M., Blazquez, M., Ribacoba, R., Salvador, C., Pastor, P., Samaranch, L., Moris, G., Menendez, M., Corao, A.I., Alvarez, V., 2010. Analysis of the Micro-RNA-133 and PITX3 genes in Parkinson's disease. *Am. J. Med. Genet. B Neurogenet. Genet.* 153B, 1234–1239. <http://dx.doi.org/10.1002/ajmg.b.31086>.
- Devine, M.J., Kaganovich, A., Ryten, M., Mamais, A., Trabzuni, D., Manzoni, C., McGoldrick, P., Chan, D., Dillman, A., Zerle, J., Horan, S., Taanman, J.W., Hardy, J., Marti-Masso, J.F., Healey, D., Schapira, A.H., Wolozin, B., Bandopadhyay, R., Cookson, M.R., van der Brug, M.P., Lewis, P.A., 2011a. Pathogenic LRRK2 mutations do not alter gene expression in cell model systems or human brain tissue. *PLoS One* 6, e22489.
- Devine, M.J., Ryten, M., Vodicka, P., Thomson, A.J., Burdon, T., Houlden, H., Cavaleri, F., Nagano, M., Drummond, N.J., Taanman, J.W., Schapira, A.H., Gwinn, K., Hardy, J., Lewis, P.A., Kunath, T., 2011b. Parkinson's disease induced pluripotent stem cells with triplication of the alpha-synuclein locus. *Nat. Commun.* 2, 440.
- Elstner, M., Morris, C.M., Heim, K., Bender, A., Mehta, D., Jaros, E., Klopstock, T., Meitinger, T., Turnbull, D.M., Prokisch, H., 2011. Expression analysis of dopaminergic neurons in Parkinson's disease and aging links transcriptional dysregulation of energy metabolism to cell death. *Acta Neuropathol.* 122, 75–86. <http://dx.doi.org/10.1007/s00401-011-0828-9>.
- Eriksen, J.L., Przedborski, S., Petrucci, L., 2005. Gene dosage and pathogenesis of Parkinson's disease. *Trends Mol. Med.* 11, 91–96. <http://dx.doi.org/10.1016/j.molmed.2005.01.001>.
- Fleige, S., Pfaffl, M.W., 2006. RNA integrity and the effect on the real-time qRT-PCR performance. *Mol. Aspects Med.* 27, 126–139. <http://dx.doi.org/10.1016/j.mam.2005.12.003>.
- Fuchs, J., Nilsson, C., Kachergus, J., Munz, M., Larsson, E.M., Schule, B., Langston, J.W., Middleton, F.A., Ross, O.A., Hulihan, M., Gasser, T., Farrer, M.J., 2007. Phenotypic variation in a large Swedish pedigree due to SNCA duplication and triplication. *Neurology* 68, 916–922. <http://dx.doi.org/10.1212/01.wnl.0000254458.17630.c5>.
- Fukuchi, M., Fujii, H., Takachi, H., Ichinose, H., Kuwana, Y., Tabuchi, A., Tsuda, M., 2010. Activation of tyrosine hydroxylase (TH) gene transcription induced by brain-derived neurotrophic factor (BDNF) and its selective inhibition through Ca(2+) signals evoked via the N-methyl-D-aspartate (NMDA) receptor. *Brain Res.* 1366, 18–26. <http://dx.doi.org/10.1016/j.brainres.2010.10.034>.
- Gasser, T., Hardy, J., Mizuno, Y., 2011. Milestones in PD genetics. *Mov. Disord.* 26, 1042–1048. <http://dx.doi.org/10.1002/mds.23637>.
- George, S., Rey, N.L., Reichenbach, N., Steiner, J.A., Brundin, P., 2013. Alpha-synuclein: the long distance runner. *Brain Pathol.* 23, 350–357. <http://dx.doi.org/10.1111/bpa.12046>.
- Gitler, A.D., Chesi, A., Geddie, M.L., Strathearn, K.E., Hamamichi, S., Hill, K.J., Caldwell, K.A., Caldwell, G.A., Cooper, A.A., Rochet, J.C., Lindquist, S., 2009. Alpha-synuclein is part of a diverse and highly conserved interaction network that includes PARK9 and manganese toxicity. *Nat. Genet.* 41, 308–315. <http://dx.doi.org/10.1038/ng.300>.
- Greene, J.G., 2011. Current status and future directions of gene expression profiling in Parkinson's disease. *Neurobiol. Dis.* 45, 76–82. <http://dx.doi.org/10.1016/j.nbd.2010.10.022>.
- Greenland, S., Morgenstern, H., 2001. Confounding in health research. *Annu. Rev. Public Health* 22, 189–212.
- Gründemann, J., Schlaudraff, F., Haackel, O., Liss, B., 2008. Elevated alpha-synuclein mRNA levels in individual UV-laser-microdissected dopaminergic substantia nigra neurons in idiopathic Parkinson's disease. *Nucleic Acids Res.* 36, e38. <http://dx.doi.org/10.1093/nar/gkn084>.
- Gründemann, J., Schlaudraff, F., Liss, B., 2011. UV-laser microdissection and mRNA expression analysis of individual neurons from postmortem Parkinson's disease brains. *Methods Mol. Biol.* 755, 363–374. http://dx.doi.org/10.1007/978-1-61779-163-5_30.
- Hardy, J., 2010. Genetic analysis of pathways to Parkinson disease. *Neuron* 68, 201–206. <http://dx.doi.org/10.1016/j.neuron.2010.10.014>.
- Harratz, M.M., Dawson, T.M., Dawson, V.L., 2011. MicroRNAs in Parkinson's disease. *J. Chem. Neuroanat.* 42, 127–130. <http://dx.doi.org/10.1016/j.jchemneu.2011.01.005>.
- Harrison, P.J., Heath, P.R., Eastwood, S.L., Burnet, P.W., McDonald, B., Pearson, R.C., 1995. The relative importance of premortem acidosis and postmortem interval for human brain gene expression studies: selective mRNA vulnerability and comparison with their encoded proteins. *Neurosci. Lett.* 200, 151–154.
- Heyer, M.P., Pani, A.K., Smeyne, R.J., Kenny, P.J., Feng, G., 2012. Normal midbrain dopaminergic neuron development and function in miR-133b mutant mice. *J. Neurosci.* 32, 10887–10894. <http://dx.doi.org/10.1523/JNEUROSCI.1732-12.2012>.
- Hindle, J.V., 2010. Ageing, neurodegeneration and Parkinson's disease. *Age Ageing* 39, 156–161. <http://dx.doi.org/10.1093/ageing/afp223>.
- Hirsch, E.C., Hunot, S., 2009. Neuroinflammation in Parkinson's disease: a target for neuroprotection? *Lancet Neurol.* 8, 382–397. [http://dx.doi.org/10.1016/S1474-4422\(09\)70062-6](http://dx.doi.org/10.1016/S1474-4422(09)70062-6).
- Ho-Pun-Cheung, A., 2009. Reverse transcription-quantitative polymerase chain reaction: description of a RIN-based algorithm for accurate data normalization. *BMC Mol. Biol.* 10, 31.
- Jowaed, A., Schmitt, I., Kaut, O., Wullner, U., 2010. Methylation regulates alpha-synuclein expression and is decreased in Parkinson's disease patients' brains. *J. Neurosci.* 30, 6355–6359. <http://dx.doi.org/10.1523/JNEUROSCI.6119-09.2010>.
- Jung, M., Schaefer, A., Steiner, I., Kempkensteffen, C., Stephan, C., Erbersdobler, A., Jung, K., 2010. Robust microRNA stability in degraded RNA preparations from human tissue and cell samples. *Clin. Chem.* 56, 998–1006. <http://dx.doi.org/10.1373/clinchem.2009.141580>.
- Junn, E., Mouradian, M.M., 2012. MicroRNAs in neurodegenerative diseases and their therapeutic potential. *Pharmacol. Ther.* 133, 142–150. <http://dx.doi.org/10.1016/j.pharmthera.2011.10.002>.

- Kalia, L.V., Kalia, S.K., McLean, P.J., Lozano, A.M., Lang, A.E., 2013. -Synuclein oligomers and clinical implications for Parkinson disease. *Ann. Neurol.* 73, 155–169. <http://dx.doi.org/10.1002/ana.23746>.
- Kalivendi, S.V., Yedlapudi, D., Hillard, C.J., Kalyanaraman, B., 2009. Oxidants induce alternative splicing of alpha-synuclein: implications for Parkinson's disease. *Free Radic. Biol. Med.* 48, 377–383. <http://dx.doi.org/10.1016/j.freeradbiomed.2009.10.045>.
- Kamp, F., Exner, N., Lutz, A.K., Wender, N., Hegemann, J., Brunner, B., Nuscher, B., Bartels, T., Giese, A., Beyer, K., Eimer, S., Winkhofer, K.F., Haass, C., 2010. Inhibition of mitochondrial fusion by alpha-synuclein is rescued by PINK1, Parkin and DJ-1. *EMBO J.* 29, 3571–3589. <http://dx.doi.org/10.1038/emboj.2010.223>.
- Kim, J., Inoue, K., Ishii, J., Vanti, W.B., Voronov, S.V., Murchison, E., Hannon, G., Abeliovich, A., 2007. A MicroRNA feedback circuit in midbrain dopamine neurons. *Science* 317, 1220–1224. <http://dx.doi.org/10.1126/science.1140481>.
- Koppelkamm, A., Vennemann, B., Lutz-Bonengel, S., Fracasso, T., Vennemann, M., 2011. RNA integrity in post-mortem samples: influencing parameters and implications on RT-qPCR assays. *Int. J. Legal Med.* 125, 573–580.
- Lesnick, T.G., Papapetropoulos, S., Mash, D.C., French-Mullen, J., Shehadeh, L., de Andrade, M., Henley, J.R., Rocca, W.A., Ahlskog, J.E., Maraganore, D.M., 2007. A genomic pathway approach to a complex disease: axon guidance and Parkinson disease. *PLoS Genet.* 3, e98. <http://dx.doi.org/10.1371/journal.pgen.0030098>.
- Li, X., Patel, J.C., Wang, J., Avshalomov, M.V., Nicholson, C., Buxbaum, J.D., Elder, G.A., Rice, M.E., Yue, Z., 2010. Enhanced striatal dopamine transmission and motor performance with LRRK2 overexpression in mice is eliminated by familial Parkinson's disease mutation G2019S. *J. Neurosci.* 30, 1788–1797. <http://dx.doi.org/10.1523/JNEUROSCI.5604-09.2010>.
- Lin, X., Parisiadou, L., Gu, X.L., Wang, L., Shim, H., Sun, L., Xie, C., Long, C.X., Yang, W.J., Ding, J., Chen, Z.Z., Gallant, P.E., Tao-Cheng, J.H., Rudow, G., Troncoso, J.C., Liu, Z., Li, Z., Cai, H., 2009. Leucine-rich repeat kinase 2 regulates the progression of neuropathology induced by Parkinson's-disease-related mutant alpha-synuclein. *Neuron* 64, 807–827. <http://dx.doi.org/10.1016/j.neuron.2009.11.006>.
- Lombardino, A.J., Li, X.C., Hertel, M., Nottebohm, F., 2005. Replaceable neurons and neurodegenerative disease share depressed UCHL1 levels. *Proc. Natl. Acad. Sci. U.S.A.* 102, 8036–8041. <http://dx.doi.org/10.1073/pnas.0503239102>.
- Lundblad, M., Decressac, M., Mattsson, B., Björklund, A., 2012. Impaired neurotransmission caused by overexpression of alpha-synuclein in nigral dopamine neurons. *Proc. Natl. Acad. Sci. U.S.A.* 109, 3213–3219.
- Mandel, S., Grunblatt, E., Riederer, P., Amariglio, N., Jacob-Hirsch, J., Rechavi, G., Youdim, M.B., 2005. Gene expression profiling of sporadic Parkinson's disease substantia nigra pars compacta reveals impairment of ubiquitin-proteasome subunits, SKP1A, aldehyde dehydrogenase, and chaperone HSC-70. *Ann. N. Y. Acad. Sci.* 1053, 356–375. <http://dx.doi.org/10.1196/annals.1344.031>.
- McCarthy, J.J., Linnertz, C., Saucier, L., Burke, J.R., Hulette, C.M., Welsh-Bohmer, K.A., Chiba-Falek, O., 2011. The effect of SNCA 3' region on the levels of SNCA-112 splicing variant. *Neurogenetics* 12, 59–64. <http://dx.doi.org/10.1007/s10048-010-0263-4>.
- McLean, J.R., Hallett, P.J., Cooper, O., Stanley, M., Isacson, O., 2011. Transcript expression levels of full-length alpha-synuclein and its three alternatively spliced variants in Parkinson's disease brain regions and in a transgenic mouse model of alpha-synuclein overexpression. *Mol. Cell Neurosci.* 49, 230–239. <http://dx.doi.org/10.1016/j.mcn.2011.11.006>.
- McNamee, R., 2005. Regression modelling and other methods to control confounding. *Occup. Environ. Med.* 62, 500–506.
- Meissner, W.G., Frasier, M., Gasser, T., Goetz, C.G., Lozano, A., Piccini, P., Obeso, J.A., Rascol, O., Schapira, A., Voon, V., Weiner, D.M., Tison, F., Bezard, E., 2011. Priorities in Parkinson's disease research. *Nat. Rev. Drug Discov.* 10, 377–393. <http://dx.doi.org/10.1038/nrd3430>.
- Mexal, S., Berger, R., Adams, C.E., Ross, R.G., Freedman, R., Leonard, S., 2006. Brain pH has a significant impact on human postmortem hippocampal gene expression profiles. *Brain Res.* 1106, 1–11. <http://dx.doi.org/10.1016/j.brainres.2006.05.043>.
- Minones-Moyano, E., Porta, S., Escaramis, G., Rabionet, R., Iraola, S., Kagerbauer, B., Espinosa-Parrilla, Y., Ferrer, I., Estivill, X., Martí, E., 2011. MicroRNA profiling of Parkinson's disease brains identifies early downregulation of miR-34b/c which modulate mitochondrial function. *Hum. Mol. Genet.* 20, 3067–3078. <http://dx.doi.org/10.1093/hmg/ddr210>.
- Mittag, F., Buchel, F., Saad, M., Jahn, A., Schulte, C., Bochtanovits, Z., Simon-Sanchez, J., Nalls, M.A., Keller, M., Hernandez, D.G., Gibbs, J.R., Lesage, S., Bace, A., Heutink, P., Martinez, M., Wood, N.W., Hardy, J., Singleton, A.B., Zöll, A., Gasser, T., Sharma, M., International Parkinson's Disease Genomics Consortium, 2012. Use of support vector machines for disease risk prediction in genome-wide association studies: concerns and opportunities. *Hum. Mutat.* 33, 1708–1718. <http://dx.doi.org/10.1002/humu.22161>.
- Moran, L.B., Duke, D.C., Deprez, M., Dexter, D.T., Pearce, R.K., Graeber, M.B., 2006. Whole genome expression profiling of the medial and lateral substantia nigra in Parkinson's disease. *Neurogenetics* 7, 1–11. <http://dx.doi.org/10.1007/s10048-005-0020-2>.
- Moran, L.B., Graeber, M.B., 2008. Towards a pathway definition of Parkinson's disease: a complex disorder with links to cancer, diabetes and inflammation. *Neurogenetics* 9, 1–13. <http://dx.doi.org/10.1007/s10048-007-0116-y>.
- Moszczynska, A., Saleh, J., Zhang, H., Vukusic, B., Lee, F.J., Liu, F., 2007. Parkin disrupts the alpha-synuclein/dopamine transporter interaction: consequences toward dopamine-induced toxicity. *J. Mol. Neurosci.* 32, 217–227.
- Nalls, M.A., Plagnol, V., Hernandez, D.G., Sharma, M., Sheerin, U.M., Saad, M., Simon-Sanchez, J., Schulte, C., Lesage, S., Sveinbjornsdottir, S., Stefansson, K., Martinez, M., Hardy, J., Heutink, P., Brice, A., Gasser, T., Singleton, A.B., Wood, N.W., 2011. Imputation of sequence variants for identification of genetic risks for Parkinson's disease: a meta-analysis of genome-wide association studies. *Lancet* 377, 641–649. [http://dx.doi.org/10.1016/S0140-6736\(10\)62345-8](http://dx.doi.org/10.1016/S0140-6736(10)62345-8).
- Opitz, L., Salinas-Riester, G., Grade, M., Jung, K., Jo, P., Emons, G., Ghadimi, B.M., Beissbarth, T., Gaedcke, J., 2010. Impact of RNA degradation on gene expression profiling. *BMC Med. Genomics* 3, 36. <http://dx.doi.org/10.1186/1755-8794-3-36>.
- Palm, T., Bahnassawy, L., Schwamborn, J., 2012. MiRNAs and neural stem cells: a team to treat Parkinson's disease? *RNA Biol.* 9, 720–730. <http://dx.doi.org/10.4161/rna.19984>.
- Pihlstrom, L., Toft, M., 2011. Genetic variability in SNCA and Parkinson's disease. *Neurogenetics* 12, 283–293. <http://dx.doi.org/10.1007/s10048-011-0292-7>.
- Pinheiro, J., Bates, D., DebRoy, S., Sarkar, D., Team, R.D.C., 2012. nlme: Linear and Nonlinear Mixed Effects Models. R package version 3.1-104.
- Polymenopoulos, M.H., Lavedan, C., Leroy, E., Ide, S.E., Dehejia, A., Dutra, A., Pike, B., Root, H., Rubenstein, J., Boyer, R., Stenroos, E.S., Chandrasekharappa, S., Athanassiadou, A., Papapetropoulos, T., Johnson, W.G., Lazzarini, A.M., Duvoisin, R.C., Di Iorio, G., Golbe, L.L., Nussbaum, R.L., 1997. Mutation in the alpha-synuclein gene identified in families with Parkinson's disease. *Science* 276, 2045–2047.
- Popova, T., Mennerich, D., Weith, A., Quast, K., 2008. Effect of RNA quality on transcript intensity levels in microarray analysis of human post-mortem brain tissues. *BMC Genomics* 9, 91. <http://dx.doi.org/10.1186/1471-2164-9-91>.
- Prasad, K., Tarasewicz, E., Strickland, P.A., O'Neill, M., Mitchell, S.N., Merchant, K., Tep, S., Hilton, K., Datwani, A., Buttini, M., Mueller-Steiner, S., Richfield, E.K., 2011. Biochemical and morphological consequences of human alpha-synuclein expression in a mouse alpha-synuclein null background. *Eur. J. Neurosci.* 33, 642–656. <http://dx.doi.org/10.1111/j.1460-9568.2010.07558.x>.
- Radi, E., Formichi, P., Di Maio, G., Battisti, C., Federico, A., 2011. Altered apoptosis regulation in kufer-rakeb syndrome patients with mutations in the ATP13A2 gene. *J. Cell Mol. Med.* 16, 1916–1923. <http://dx.doi.org/10.1111/j.1582-4934.2011.01488.x>.
- Ramirez, A., Heimbach, A., Grundemann, J., Stiller, B., Hampshire, D., Cid, L.P., Goebel, I., Mubaidin, A.F., Wriekat, A.L., Roeper, J., Al-Din, A., Hillmer, A.M., Karsak, M., Liss, B., Woods, C.G., Behrens, M.L., Kubisch, C., 2006. Hereditary parkinsonism with dementia is caused by mutations in ATP13A2, encoding a lysosomal type 5 P-type ATPase. *Nat. Genet.* 38, 1184–1191. <http://dx.doi.org/10.1038/ng1884>.
- Ransdell, J.L., Faust, T.B., Schulz, D.J., 2010. Correlated levels of mRNA and soma size in single identified neurons: evidence for compartment-specific regulation of gene expression. *Front. Mol. Neurosci.* 3, 116. <http://dx.doi.org/10.3389/fnmol.2010.00116>.
- Reddy, S.D., Rayala, S.K., Ohshiro, K., Pakala, S.B., Kobori, N., Dash, P., Yun, S., Qin, J., O'Malley, B.W., Kumar, R., 2011. Multiple coregulatory control of tyrosine hydroxylase gene transcription. *Proc. Natl. Acad. Sci. U.S.A.* 108, 4200–4205. <http://dx.doi.org/10.1073/pnas.110193108>.
- Salmena, L., Poliseno, L., Tay, Y., Kats, L., Pandolfi, P.P., 2011. A ceRNA hypothesis: the Rosetta Stone of a hidden RNA language? *Cell* 146, 353–358. <http://dx.doi.org/10.1016/j.cell.2011.07.014>.
- Scherzer, C.R., Jensen, R.V., Gullans, S.R., Feany, M.B., 2003. Gene expression changes presage neurodegeneration in a Drosophila model of Parkinson's disease. *Hum. Mol. Genet.* 12, 2457–2466. <http://dx.doi.org/10.1093/hmg/ddg265>.
- Schulz, D.J., Goillard, J.M., Marder, E.E., 2007. Quantitative expression profiling of identified neurons reveals cell-specific constraints on highly variable levels of gene expression. *Proc. Natl. Acad. Sci. U.S.A.* 104, 13187–13191. <http://dx.doi.org/10.1073/pnas.0705827104>.
- Schwarz, G., 1978. Estimating the dimension of a Model. *Ann. Statist.* 6, 461–464.
- Shulman, J.M., De Jager, P.L., Feany, M.B., 2011. Parkinson's disease: genetics and pathogenesis. *Annu. Rev. Pathol.* 6, 193–222. <http://dx.doi.org/10.1146/annurev-pathol-011110-130242>.
- Simunovic, F., Yi, M., Wang, Y., Macey, L., Brown, L.T., Krichevsky, A.M., Andersen, S.L., Stephens, R.M., Benes, F.M., Sonntag, K.C., 2009. Gene expression profiling of substantia nigra dopamine neurons: further insights into Parkinson's disease pathology. *Brain* 132 (Pt 7), 1795–1809. <http://dx.doi.org/10.1093/brain/awn323>.
- Snijders, T.A., Bosker, R., 2011. *Multilevel Analysis: An Introduction to Basic and Advanced Multilevel Modeling*, second ed. Sage, London.
- Sonntag, K.C., 2010. MicroRNAs and deregulated gene expression networks in neurodegeneration. *Brain Res.* 1338, 48–57. <http://dx.doi.org/10.1016/j.brainres.2010.03.106>.
- Spillantini, M.G., Schmidt, M.L., Lee, V.M., Trojanowski, J.Q., Jakes, R., Goedert, M., 1997. Alpha-synuclein in Lewy bodies. *Nature* 388, 839–840. <http://dx.doi.org/10.1038/42166>.
- Stahlberg, A., Andersson, D., Aurelius, J., Faiz, M., Pekna, M., Kubista, M., Pekny, M., 2011. Defining cell populations with single-cell gene expression profiling: correlations and identification of astrocyte subpopulations. *Nucleic Acids Res.* 39, e24. <http://dx.doi.org/10.1093/nar/gkq1182>.
- Tang, F., Lao, K., Surani, M.A., 2011. Development and applications of single-cell transcriptome analysis. *Nat. Methods* 8 (4 Suppl), S6–S11. <http://dx.doi.org/10.1038/nmeth.1557>.
- Tobin, A.E., Cruz-Bermudez, N.D., Marder, E., Schulz, D.J., 2009. Correlations in ion channel mRNA in rhythmically active neurons. *PLoS One* 4, e6742. <http://dx.doi.org/10.1371/journal.pone.0006742>.
- Ugolino, J., Fang, S., Kubisch, C., Monteiro, M.J., 2011. Mutant Atp13a2 proteins involved in parkinsonism are degraded by ER-associated degradation and sensitize cells to ER-stress induced cell death. *Hum. Mol. Genet.* 20, 3565–3577. <http://dx.doi.org/10.1093/hmg/ddr274>.

- Vartiainen, S., Pehkonen, P., Lakso, M., Nass, R., Wong, G., 2006. Identification of gene expression changes in transgenic *C. elegans* overexpressing human alpha-synuclein. *Neurobiol. Dis.* 22, 477–486. <http://dx.doi.org/10.1016/j.nbd.2005.12.021>.
- Venda, L.L., Cragg, S.J., Buchman, V.L., Wade-Martins, R., 2010. -Synuclein and dopamine at the crossroads of Parkinson's disease. *Trends Neurosci.* 33, 559–568. <http://dx.doi.org/10.1016/j.tins.2010.09.004>.
- Vermeulen, J., De Preter, K., Lefever, S., Nuytens, J., De Vloed, F., Derveaux, S., Hellemans, J., Speleman, F., Vandesompele, J., 2011. Measurable impact of RNA quality on gene expression results from quantitative PCR. *Nucleic Acids Res.* 39, e63. <http://dx.doi.org/10.1093/nar/gkr065>.
- Volpicelli, F., De Gregorio, R., Pulcrano, S., Perrone-Capano, C., di Porzio, U., Bellenchi, G.C., 2012. Direct regulation of Pitx3 expression by Nurr1 in culture and in developing mouse midbrain. *PLoS One* 7, e30661. <http://dx.doi.org/10.1371/journal.pone.0030661>.
- Wang, G., van der Walt, J.M., Mayhew, G., Li, Y.J., Zuchner, S., Scott, W.K., Martin, E.R., Vance, J.M., 2008. Variation in the miRNA-433 binding site of FGF20 confers risk for Parkinson disease by overexpression of alpha-synuclein. *Am. J. Hum. Genet.* 82, 283–289. <http://dx.doi.org/10.1016/j.ajhg.2007.09.021>.
- Yasuda, T., Nihira, T., Ren, Y.R., Cao, X.Q., Wada, K., Setsuie, R., Kabuta, T., Hattori, N., Mizuno, Y., Mochizuki, H., 2009. Effects of UCH-L1 on alpha-synuclein overexpression mouse model of Parkinson's disease. *J. Neurochem.* 108, 932–944. <http://dx.doi.org/10.1111/j.1471-4159.2008.05827.x>.
- Yeger-Lotem, E., Riva, L., Su, L.J., Gitler, A.D., Cashikar, A.G., King, O.D., Auluck, P.K., Geddie, M.L., Valastyan, J.S., Karger, D.R., Lindquist, S., Fraenkel, E., 2009. Bridging high-throughput genetic and transcriptional data reveals cellular responses to alpha-synuclein toxicity. *Nat. Genet.* 41, 316–323. <http://dx.doi.org/10.1038/ng.337>.
- Youle, R.J., Narendra, D.P., 2011. Mechanisms of mitophagy. *Nat. Rev. Mol. Cell Biol.* 12, 9–14.
- Zhang, Y., James, M., Middleton, F.A., Davis, R.L., 2005. Transcriptional analysis of multiple brain regions in Parkinson's disease supports the involvement of specific protein processing, energy metabolism, and signaling pathways, and suggests novel disease mechanisms. *Am. J. Med. Genet. B Neuropsychiatr. Genet.* 137B, 5–16. <http://dx.doi.org/10.1002/ajmg.b.30195>.
- Zhou, Z., Kim, J., Insolera, R., Peng, X., Fink, D.J., Mata, M., 2011. Rho GTPase regulation of alpha-synuclein and VMAT2: implications for pathogenesis of Parkinson's disease. *Mol. Cell Neurosci.* 48, 29–37. <http://dx.doi.org/10.1016/j.mcn.2011.06.002>.
- Ziebell, M., Khalid, U., Klein, A.B., Aznar, S., Thomsen, G., Jensen, P., Knudsen, G.M., 2010. Striatal dopamine transporter binding correlates with serum BDNF levels in patients with striatal dopaminergic neurodegeneration. *Neurobiol. Aging* 33, 428.e1–428.e5. <http://dx.doi.org/10.1016/j.neurobiolaging.2010.11.010>.